Moving Boundary Transport Phenomena in Selective Area Laser Deposition Process

Guisheng Zong and Harris L. Marcus

Center for Materials Science & Engineering
The University of Texas at Austin
Austin, Texas 78712

Abstract

The overall selective area laser deposition process was modeled using the two-layer, three dimensional solid phase heat transfer with the moving boundary condition considered, gas phase mass transfer, and film growth coupled equations. A modified front-tracking finite difference method was used to solve the moving boundary heat conduction in thick deposits. The results correlate with the experimental observations.

1. Introduction

The present state of modeling selective area pyrolytic laser deposition is far from complete because modeling microreaction is a complex, multifaceted problem. In the initial modeling Jacquot, Zong and Marcus [1] used a finite difference technique to model pyrolytic SALD of a carbon film on alumina substrate from acetylene using a focused CO_2 laser. A temperature-dependent thermal conductivity and a deposit reflectivity which changes as the film grows were included in the model, while the deposit solid phase heat conduction (important in determining the time - varying local temperature profile) was excluded. The model is essentially a model for laser-induced pyrolytic CVD of thin films, as found in the literature [2-4]. It only has limited applicability to model the thick film SALD process. In the case of SALD it turns out to be essential to consider the heat transport through the deposited material, especially when the thermal conductivity of the substrate is much smaller than that of the deposits. A deposited metal strip of, for example, unit aspect ratio (height/width) serves as an efficient thermal sink on a poorly conducting substrate yielding a surface temperature less than expected for a flat surface [5]. Conversely, a very high aspect ratio is thermally decoupled from the heat sink of the substrate and its surface temperature rises. In this research the overall SALD process was modeled and a code was developed on the Cray supercomputer.

2. The Physical Picture

The model describes the growth of a three-dimensional object on a substrate by selective area pyrolytic laser deposition, including the solid-phase, substrate and deposit, heat conduction, gas-phase mass transfer, and the growth of the film. Deposit nucleation was not considered. Temperature-dependent parameters are used. Most of the modeling equations to be described are general, but to do the calculations a sample system with specific parameter values was considered. The sample system considered is the pyrolytic deposition of carbon from acetylene by the overall reaction

$$C_2H_2 \text{ (g)} + \Delta E \Leftrightarrow 2C \text{ (s)} + H_2 \text{ (g)} \tag{1}$$

A Gaussian-shaped laser beam of wavelength 10.6μm is used. A finite alumina substrate is

assumed in the model. This then allows comparison to the experimental data obtained. Mass transport to the surface by convection is neglected in the region of interest, so the reactant transport to and from the surface occurs only by diffusion.

2.1 Solid-phase heat transport

In the pyrolytic SALD process, the temperature field has to be obtained to determine the chemical reaction zone on the surface of the substrate or the overlaying deposit. Figure 1 shows the geometry of the problem to be solved and the coordinate system under considerations. The deposit with a thickness as a function of position and time is on a substrate of dissimilar material. The materials are assumed to be isotropic and finite in size.
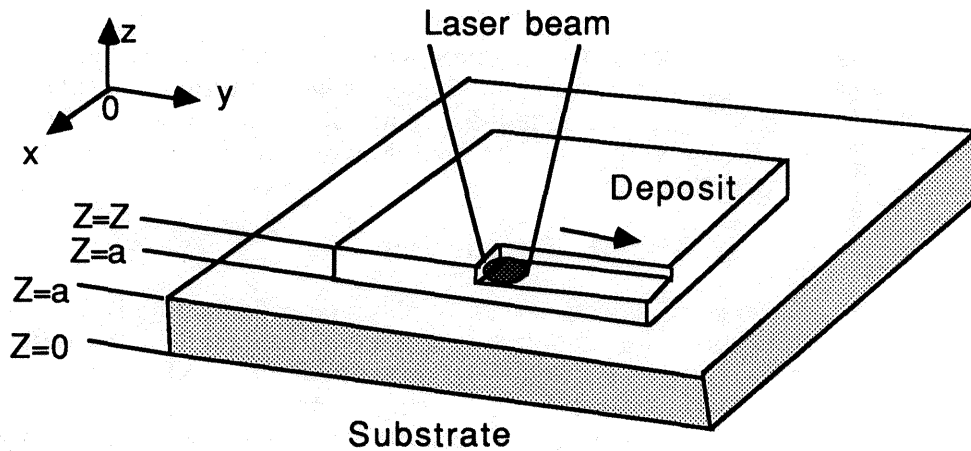
Fig. 1 Geometry used in the present modeling

The heat transfer equation for an isotropic medium is

$$\frac{k(T)}{D(T)} \frac{\partial T(x,y,z,t)}{\partial t} - \nabla[k(T)\nabla T(x,y,z,t)] = Q$$

(2)

where $k(T)$ and $D(T)$ are the temperature-dependent conductivity and the thermal diffusivity, respectively. $T(x,y,z,t)$ is the temperature at point (x,y,z) in Cartesian coordinates at time t. ∇ is the three-dimensional del operator. The heat source term is the sum of the heat from laser beam, the radiative/ convective heat losses, and the heat supplied locally by the chemical reaction.

$$Q = [P_{laser}(1-R)/\pi w^2] \exp[-(x^2 + y^2)/w^2] + (A_0 sn)\Delta G$$

$$- [h(T(x,y) - T_{out}) + \sigma \varepsilon_0(T^4(x,y) - T^4_{out})]$$

(3)

where P_{laser} is the incident laser power on the substrate, R is the surface reflectivity, and w the laser beam waist, n is the atomic density of the deposit, ΔG is the free energy per atom deposited, A_0 is the cross section of the material deposited with a scan speed of s, h is the convective heat transfer coefficient, σ is the Stefan-Boltzmann constant, ε_0 is the hemispherical total emittance at temperature T, and T_{out} is the ambient temperature.

In the SALD process, heat transfer in two different stages, thin films and thicker deposits,

have to be considered.

Thin film stage

Ideally, the deposit should always be included in the solid-phase heat conduction, but due to the thinness of the deposit in the early stage of SALD process, the time steps for the numerical analysis become too small, and the two-layer problem becomes numerically stiff. Therefore, the thin film is treated as an intensity filter for the substrate, modifying the laser intensity by changing in the surface reflectivity.

The surface reflectivity is expresses as a function of the deposit thickness in the form [4]

$$R(x,y) = R_1 + (R_2 - R_1) \exp [- gl (x,y)] \tag{4}$$

where

R_1=reflectivity of bulk deposit material =0.2 for graphite
R_2=reflectivity of substrate material =0.8 for alumina.

l is the thickness of deposit, and g is an empirical characteristic attenuation parameter. The temperature profile can be obtained by solving equation (2). The substrate is assumed to be a finite slab and therefore the boundary conditions applicable to equation (2) are given by convective and radiative heat losses through the surface of the substrate. The initial conditions at t=0 are

Substrate Temperature Distribution: STD $(x,y,z) = T_0$
Carbon Deposit Thickness: CDT $(x,y) = 0$,
Acetylene Concentration Distribution: ACD $(x,y,z) = C_0$.

Thicker deposits stage

When the deposit thickness is equal to g the thick film analysis is used. The heat equations to be solved for the deposit and the substrate of thickness a can be written as

$$\frac{k_d(T_d)}{D_d(T_d)} \frac{\partial T_d}{\partial t} - \nabla[k_d(T_d)\nabla T_d] = Q \qquad \text{for } z>a, \tag{5}$$

$$\frac{k_s(T_s)}{D_s(T_s)} \frac{\partial T_s}{\partial t} - \nabla[k_s(T_s)\nabla T_s] = 0 \qquad \text{for } z<a, \tag{6}$$

where the subscripts d and s denote the values for deposit and substrate. At the interface between the deposit and the substrate, the boundary conditions come from energy conservation for heat flow and temperature continuity:

$$k_d(T_d) \frac{dT_d}{dz} = k_s(T_s) \frac{dT_s}{dz} \qquad \text{at } z=a, \tag{7}$$

$$T_d=T_s \qquad \text{at } z=a. \tag{8}$$

2.2 Gas-phase mass transport

The mass transfer equation is given by:

$$v\nabla C_i + \frac{\partial C_i}{\partial t} = D_i \nabla^2 C_i + R_i \tag{9}$$

With no bulk motion, $v = 0$. R_i is the source term. We assume that the temperature of the gas is constant and equal to T_{gas}. Using the perfect gas equation in a fixed volume, we find the relation between P_{C2H2} and C_{C2H2}:

$$P_{C2H2} = C_{C2H2} \, R_g \, T_{gas} \tag{10}$$

where R_g is the gas constant.

2.3 The carbon deposition rate

Leyendecker et al. have determined the apparent activation energy for the reaction (1) using a laser induced chemical vapor deposition setup [6]. Their result for the case of pyrolytic carbon which was deposited from acetylene at various gas pressure is

$$\Delta E_a = 213 \pm 8 \text{ KJ/mole}$$

This value also correlates some other literature values [7]. We fit their data using the minimization of the coefficient of least squares method to obtain a linear growth rate equation

$$\frac{dl}{dt} = \exp\left[\frac{\Delta E}{k} \, (5.86 * 10^{-4} - \frac{1}{T})\right] \, [P_{C_2H_2}]^\alpha \quad \mu ms^{-1} \tag{11}$$

where k is the Boltzmann constant and $\alpha = \left[\frac{10^{-4}}{\ln 10} \frac{\Delta E}{k}\right] = 1.02$. Equation (11) was used to calculate the carbon deposition profile in this study.

3. Numerical Procedure

In order to solve the nonlinear heat equations (2), (5), and (6), the Kirchhoff transform [7,8] is applied to eliminate the temperature-dependent thermal conductivity k(T) from the heat equation. The Kirchhoff transform requires the introduction of a linearized temperature Θ, which is defined as

$$\Theta(T) = \Theta(T_0) + \int_{T_0}^{T} \frac{k(T')}{k(T_0)} \, dT' \tag{12}$$

where $\Theta(T_0)$ and $k(T_0)$ are constants.

The heat transfer equation (2) can be now written in terms of the linearized temperature Θ as

$$\frac{1}{D(T(\Theta))} \frac{\partial \Theta}{\partial t} - \nabla^2 \Theta = \frac{Q}{k(T_0)} \tag{13}$$

which can be solved by a finite difference method.

By applying Kirchhoff transform to the equations in the thick deposit case, equations (5)-(8) can be written in terms of the linearized temperature Θ_d and Θ_s:

$$\frac{1}{D_d(T_d(\Theta_d))} \frac{\partial \Theta_d}{\partial t} - \nabla^2 \Theta_d = \frac{Q}{k_d(T_0)} \qquad \text{for } z>a \tag{14}$$

282

$$\frac{1}{D_s(T_s(\Theta_s))} \frac{\partial \Theta_s}{\partial t} - \nabla^2 \Theta_s = 0 \qquad \text{for } z<a \qquad (15)$$

$$k_d(T_a)\frac{d\Theta_d}{dz} = k_s(T_a)\frac{d\Theta_s}{dz} \qquad \text{at } z=a \qquad (16)$$

$$\Theta_d = \Theta_s \qquad \text{at } z=a \qquad (17)$$

A moving grid system (Figure 2), which was first used by Crank and Gupta [10,11] for a one-dimensional problem, arising from the diffusion of oxygen in absorbing tissue, is used to solve equation (14) under moving boundary conditions. The deposit is subdivided into n intervals each of width Δz such that $z = i\Delta z + a$; $i=0,1,...,n$ ($n\Delta z=l$) at $t=0$. As the boundary moves a distance Δl at the next time step Δt the whole grid system is moved a distance Δl from the fixed surface (substrate surface) $z=a$. The size of the first interval will then increase to $\Delta z + \Delta l = z^1$ and in general if the position of the ith mesh point at $t=j\Delta t$ is z_i^j, then

$$z_i^j = z^j + (i-1)\Delta z + a, \qquad i=1,2, \ldots , \qquad (18)$$

$$z_i^{j+1} = z_i^j + \Delta l^{j+1} + a, \qquad (19)$$

$$z^{j+1} = z^j + \Delta l^{j+1} + a, \qquad (20)$$

where Δl^{j+1} is the thickness deposited from time $j\Delta t$ to $(j+1)\Delta t$.
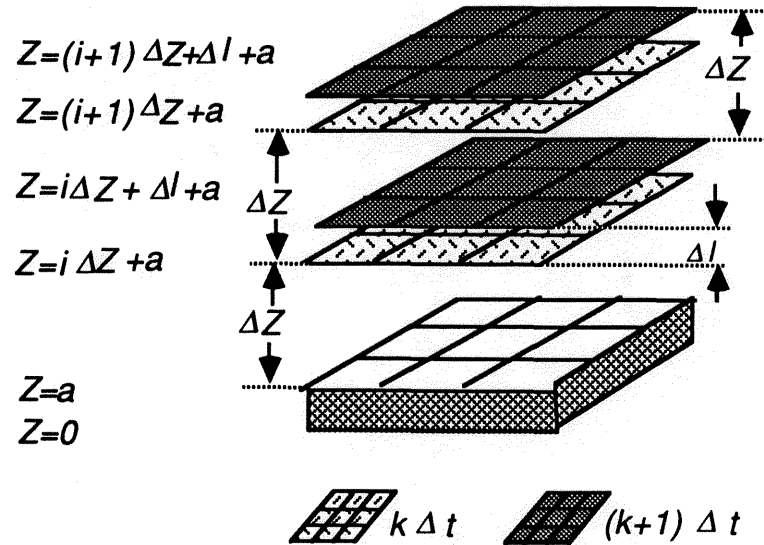
Fig. 2 Moving grid system

By using the Taylor's series for Θ and neglecting higher derivatives, we have

$$\Theta(x,y,z+\Delta l,t+\Delta t) = \Theta(x,y,z,t) + \Delta l\frac{\partial \Theta}{\partial z} + \frac{\Delta l^2}{2}\frac{\partial^2 \Theta}{\partial z^2}$$
$$+ \Delta t D(T)\left[\nabla^2\Theta + \frac{Q}{k(T_0)}\right] \qquad (21)$$

At the grid point z=ζ Lagrange type formula have to be used allowing for the unequal interval z nearest to the surface x=a. The respective equations are

$$\Theta'_{i,j,1} = \frac{\zeta \Theta_{i,j,2}}{\Delta z(\zeta + \Delta z)} - \frac{(\Delta z - \zeta)\Theta_{i,j,1}}{\zeta \Delta z} + \frac{\Delta z \Theta_{i,j,0}}{\zeta(\zeta + \Delta z)}\}$$

(22)

$$\Theta''_{i,j,1} = 2\left\{ \frac{\Theta_{i,j,2}}{\Delta z(\zeta + \Delta z)} - \frac{\Theta_{i,j,1}}{\zeta \Delta z} + \frac{\Theta_{i,j,0}}{\zeta(\zeta + \Delta z)}\right\}$$

(23)

The temperature at any time step is calculated from (21) using (22) and (23).

4. Results and Discussion

The model described above can be used to carry out parametric studies of the SALD process. Some typical results are presented in this section.

Figures 3(a) and 3(b) represent the temperature distribution on the top surface of the substrate for laser power, P=5W and laser scanning speed relative to the substrate, s=0.1 and 10 mm/s respectively. It can be seen from these figures that the shape of the surface temperature field has a Gaussian structure, modified by the scanning speed of the laser beam, due to the consideration of the Gaussian laser beam as the heat source. The peak temperature decreases from 1994 ^{0}K to 1876 ^{0}K as scanning speed increased from 0.1 mm/s to 10 mm/s. The size of the laser heated zone also decreases as laser scanning speed increased, due to the dwell time effect. The knowledge of the width of the laser heated zone is very important in SALD. The laser heated zone controls the resolution of the SALD and the definition of the products. The chemical reaction that generates the film forming material will take place wherever the temperature is more than or equal to the chemical reaction temperature. Thus, the resolution in the SALD process can be controlled by adjusting scanning speed.
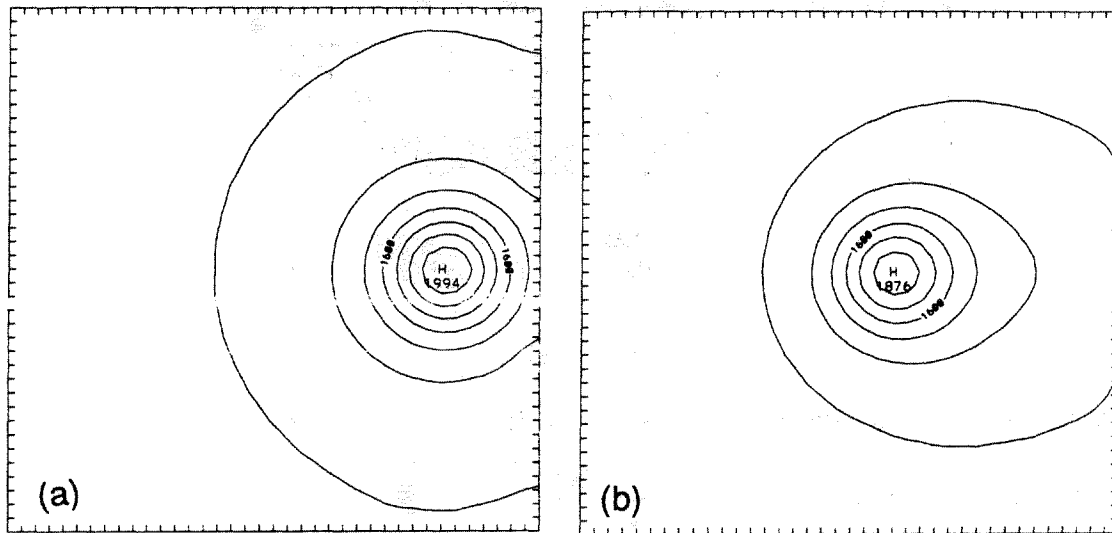
Figure 3 Surface temperature distribution for the laser beam of power 5W and scanning at a speed (a) 0.1 mm/s and (b) 10 mm/s.

Laser power is another process parameter that can be used to control the resolution in the SALD. Figure 4 clearly shows this control ability. The width of the stripe in Fig. 4(a) is obvious less than that in Fig. 4(b) due to the laser power change from 8W to 12 W, indicating that increasing the laser power decreases the resolution.

Figure 4 also show that the width and thickness of the stripe deposited increase as time increases. This is because at slow scanning speed the conduction rate is higher than the heat storage rate. Consequently, the substrate material which is in front of the laser beam is heated up due to the heat conducted away from the laser heated spot. Hence, the laser energy is progressively imparted to points on the substrate which are at higher temperatures than the preceding points. For the very same reason, the laser heated zone in the other directions on the substrate increases as time increases for low scanning speed. Thus, the film width will not be uniform for low scanning speed. Figure 5 shows the correlation between a partial line scan experimental result and the modeling result.
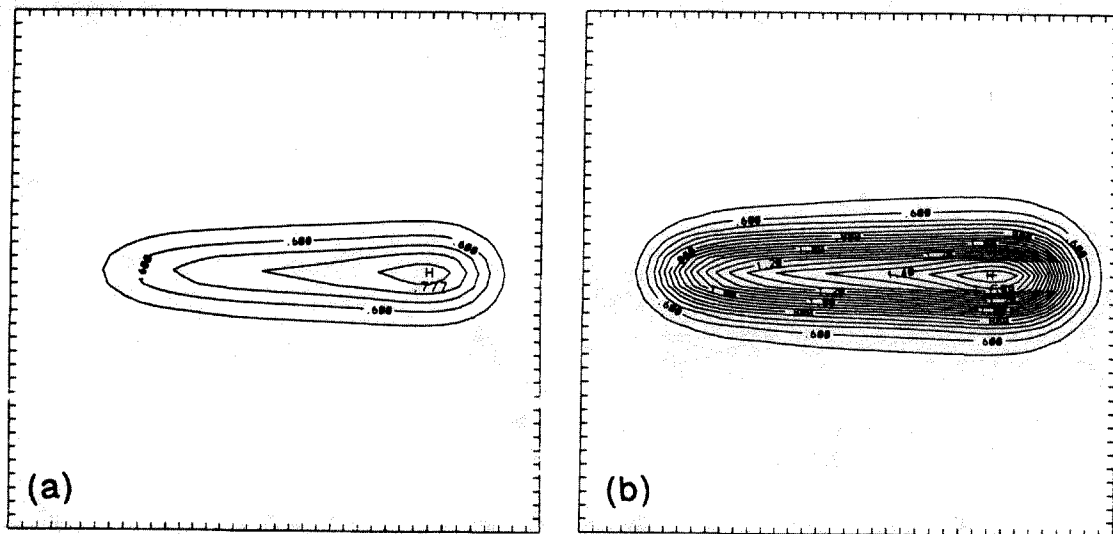
Figure 4 Carbon deposition profile for the laser beam of power (a) 8W and (b) 12W and scanning at a speed 1 mm/s.
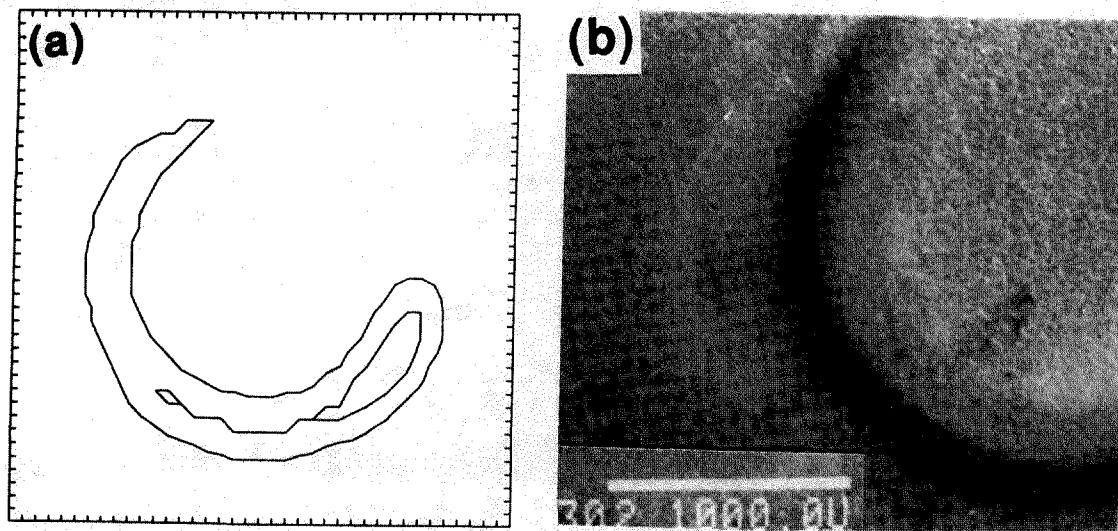
Figure 5 Comparison of carbon deposition simulation profile (a) with a single scan carbon deposit on alumina substrate (b). (Acetylene pressure 200 Torr, laser power 8W, scanning speed 42μm/s).

On the other hand, if the scanning speed is high the conduction rate will be lower than the heat storage rate. This reduces the area of the chemically reactive zone due to less heat conduction of heat from the laser heated spot. Because of this, SALD of constant width film can be deposited on the substrate by increasing the scanning speed of the laser beam, as shown in Figure 6. The stripe in Figure 6 is modeled in the same process conditions as in the Figure 4(a) except the scanning speed is 10 mm/s instead of 1 mm/s.
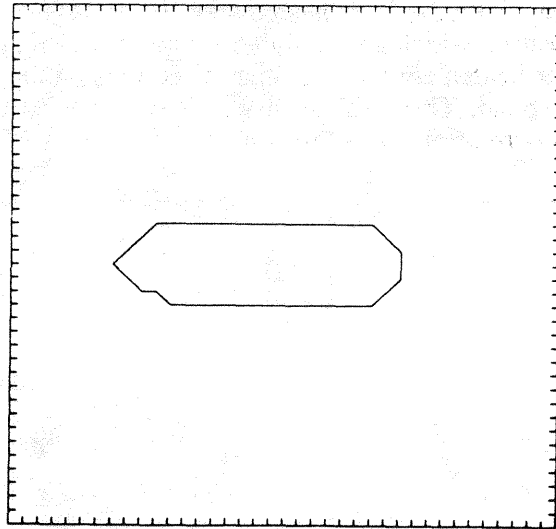
Figure 6 Carbon deposition profile for the laser beam of power 8W and scanning at a speed 10 mm/s.

The calculation also showed that the deposit acted as heat sink which lowered the peak temperature for a given laser power for thick film deposition [12]. With moving boundary condition and heat transfer in the deposit considered, the model gives more accurate predictions.

5. Summary

The mathematical model proposed predicts laser-induced temperature profiles both in substrates and in thick deposits and the thickness of carbon layers deposited by selective area laser decomposition of acetylene and correlates with the experimental results. Future modeling will continue taking into account more complex chemical reactions and chemically reacting gas flows with nonuniform flow and temperature fields involved in the selective area laser deposition.

Acknowledgement

Reference

1. Y. Jacquot, G. Zong, and H.L. Marcus, "Modeling of selective area laser deposition for solid freeform fabrication," Proceedings of The Solid Freeform Fabrication Symposium, Edited by J.J. Beaman, H.L. Marcus, D.L. Bourell, and J.W. Barlow, Austin, Texas, August 6-8, 1990, 74-82.
2. A. Kar and J. Mazumder, "Three-dimensional transient thermal analysis for laser chemical

vapor deposition on uniformly moving finite slabs," J. Appl. Phys., 65(8), 1989, 2923-2934.

3. D. C. Skouby and K. F. Jensen, "Modeling of pyrolytic laser-assisted chemical vapor deposition: Mass transfer and kinetic effects influencing the shape of the deposit," J. Appl. Phys., 63(1), 1988, 198-206.

4. J. E. Moody and R. H. Hendel, "Temperature profiles induced by a scanning cw laser beam," J. Appl. Phys., 53(6), 1982, 4364-4371.

5. K. Piglmayer, J. Doppelbauer, and D. Bäuerle, "Temperature distributions in cw laser induced pyrolytic deposition," Mat. Res. Soc. Symp. Proc., 29, 1984, 47-54.

6. G. Leyendecker, H. Noll, D. Bäuerle, P. Geittner, and H. Lydtin, "Rapid determination of apparent activation energies in chemical vapor deposition," J. Electrochem Soc: Solid-state science and technology, 130(1), 157-160.

7. Y. Schwob, "Acetylene black," Chemistry and physics of carbon, 15, 1979, 124.

8. H. S. Carslaw and J. C. Jaeger, "Conduction of heat in solids," Oxford, Clarendon press, 1959, 10-11.

9. E.R.G. Eckert, "Analysis of heat and mass transfer," Hemisphere Publishing Corporation, 1987, 9-12.

10. J. Crank and R.S. Gupta, "A method for solving moving boundary problems in heat flow using cubic splines or polynomials," J. Inst. Maths Applics 10, 1972, 269-304.

11. J. Crank, "Free and moving boundary problems," Clarendon Press, Oxford, 1984, 163-186.

12. G. Zong, "Solid freeform fabrication using selective area laser deposition," Ph.D. Thesis, The University of Texas at Austin, August 1991.